Physics Letters B 735 (2014) 168–172

Contents lists available at ScienceDirect

Physics Letters B

www.elsevier.com/locate/physletb

The next-to-leading order vertex for a forward jet plus a rapidity gap at high energies

M. Hentschinski [a], J.D. Madrigal Martínez [b,*], B. Murdaca [c,d], A. Sabio Vera [e,f,g]

[a] Department of Physics, Brookhaven National Laboratory, Upton, NY 11973, USA
[b] Institut de Physique Théorique, CEA Saclay, F-91191 Gif-sur-Yvette, France
[c] Dipartimento di Fisica, Università della Calabria, I-87036 Arcavacata di Rende, Cosenza, Italy
[d] Istituto Nazionale di Fisica Nucleare, Gruppo Collegato di Cosenza, I-87036 Arcavacata di Rende, Cosenza, Italy
[e] Instituto de Física Teórica UAM/CSIC, Nicolás Cabrera 15, E-28049 Madrid, Spain
[f] U. Autónoma de Madrid, E-28049 Madrid, Spain
[g] CERN, Geneva, Switzerland

ARTICLE INFO

Article history:
Received 21 April 2014
Received in revised form 30 May 2014
Accepted 8 June 2014
Available online 12 June 2014
Editor: G.F. Giudice

ABSTRACT

We present the results for the calculation of the forward jet vertex associated to a rapidity gap (coupling of a hard pomeron to the jet) in the Balitsky–Fadin–Kuraev–Lipatov (BFKL) formalism at next-to-leading order (NLO). We handle the real emission contributions making use of the high energy effective action proposed by Lipatov, valid for multi-Regge and quasi-multi-Regge kinematics. This result is important since it allows, together with the NLO non-forward gluon Green function, to perform NLO studies of jet production in diffractive events (Mueller–Tang dijets, as a well-known example).

1. Introduction

In recent years we have developed useful techniques [1] to work with the high energy effective action proposed by Lev Lipatov [2] to calculate scattering amplitudes relevant in the multi-Regge limit. This action is based on the separation of the emitted particles into clusters widely apart in rapidity. These clusters are connected to each other by reggeized gluon propagators which act as non-Sudakov form factors generating regions in rapidity with no emissions. The value of the effective action is to account for the interactions of these reggeized gluons with usual quarks and gluons inside the emission clusters. The strong ordering in rapidity among the clusters allows for the efficient resummation of powers of rapidity, or large logarithms in the center-of-mass energy, which are present in the scattering amplitudes. Of course, the coefficients of these logarithms are correctly calculated when compared to exact evaluations of the scattering amplitudes, both in elastic and complicated inelastic cases.

There are at least two technical details which we need to treat with care in this program. One of them is to avoid double counting when considering that some emissions are inside the cluster or in a neighboring one. For this we have introduced a subtraction and regularization method. The second complication is at loop level since the effective action is formulated in terms of non-local operators which introduce new ultraviolet divergencies which are not related to short distance physics but have a kinematical origin. In this case we introduce a cut-off in the loop integrations which we have proven to be related to powers of total rapidity. This cut-off can be interpreted as a small deformation of the light cone. This is a delicate procedure, specially when one needs to perform two or higher loop calculations since the integrals we encounter are not of the standard types investigated in the literature.

Our proposed methods have been tested in well-known quantities. At two loop level we have successfully reproduced the gluon Regge trajectory at NLO, first the simpler quark contributions [3] and then the more complicated gluon ones [4]. At one loop level with inelastic amplitudes we have calculated the jet vertex for the production of a jet in the forward direction coupled to a reggeized gluon [5]. This configuration has minijet radiation associated to the forward jet and it is used in the calculation of the so-called Mueller–Navelet cross sections [6] which are playing an important role in the application of the BFKL formalism [7] to phenomenology at the Large Hadron Collider (LHC). In this case again the quark-initiated jets are simpler to evaluate than the gluon-initiated ones.

Our present target is to evaluate the NLO contributions to the production of a forward jet this time coupled to a bound state of two reggeized gluons, or hard pomeron, which lives in a color singlet representation and does not have associated minijet radiation but a rapidity gap instead. The calculation is also divided into quark and gluon initiated jets and has numerous applications in

* Corresponding author.

http://dx.doi.org/10.1016/j.physletb.2014.06.022

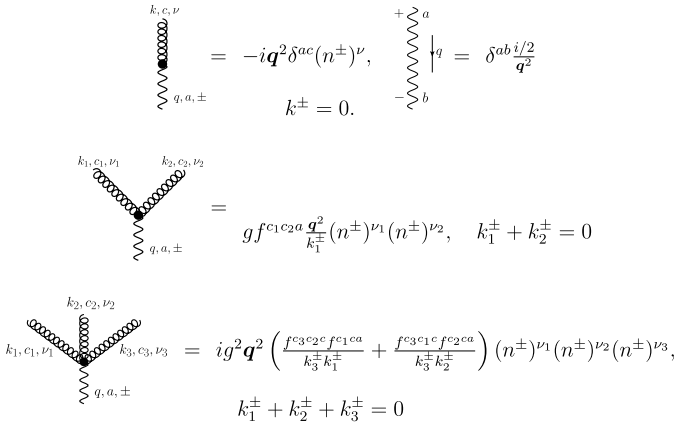

Fig. 1. Feynman rules for the lowest-order effective vertices of the effective action [10]. Wavy lines denote reggeized fields and curly lines gluons. Pole prescriptions for the light-cone denominators are discussed in [11].

the field of diffractive jet production, the most famous one being Mueller–Tang jet production [8]. In this observable two jets are emitted in the forward direction of each hadron and a large rapidity gap sits in between them.

Technically, this calculation is rather involved and in this letter we present the final results to be used for phenomenology. In separate publications [9] we will show the detailed evaluation of both the quark and gluon initiated components. We first make a nutshell presentation of the high energy effective action indicating the relevant effective Feynman rules which are needed in our calculation. Then we introduce the notation to understand the relevant variables present in the description of the jet vertex, to finally describe our results and discuss directions for future theoretical and phenomenological studies.

2. Basics of the high energy effective action

We are interested in dijet production in hadron–hadron collisions at very high energies, $p(p_A)+p(p_B)\to J_1(p_{J,1})+J_2(p_{J,2})+$ gap, where there exists a large region in rapidity Δy_{gap} in between the tagged jets without hadronic activity. In perturbative QCD we understand this rapidity gap as generated by a color singlet exchange in the t-channel which takes the form of a hard or BFKL pomeron whose interactions with external particles are well described by Lipatov's high energy effective action [2]. To the usual QCD action we add an extra piece which accounts for the interaction of reggeized t-channel gluons (reggeons) and normal quarks and gluons: $S_{\text{eff}} = S_{\text{QCD}} + S_{\text{ind}}$. The extra "induced" piece reads

$$S_{\text{ind}} = \int \mathrm{d}^4x \,\mathrm{Tr}\big[\big(W_-\big[v(x)\big] - A_-(x)\big)\partial_\perp^2 A_+(x) + \{+\leftrightarrow -\}\big], \quad (1)$$

where $v_\mu = -iT^a v_\mu^a(x)$ is the gluon field, and $A_\pm(x) = -iT^a A_\pm^a(x)$ is the reggeon field, introduced as a new degree of freedom, which mediates any interaction between clusters of emitted particles well separated in rapidity.

Locally in rapidity, within each cluster, the reggeon–gluon interactions are mediated by the Wilson line couplings

$$W_\pm\big[v(x)\big] = -\frac{1}{g}\partial_\pm \mathcal{P}\exp\left\{-\frac{g}{2}\int_{-\infty}^{x^\mp} \mathrm{d}z^\pm v_\pm(z)\right\}. \quad (2)$$

The reggeon field satisfies the kinematic constraint $\partial_\pm A_\mp(x) = 0$ which is present in the Feynman rules of Fig. 1. We use the Sudakov decomposition $k = k^+n^-/2 + k^-n^+/2 + \boldsymbol{k}$ where $n^\pm = 2p_{A,B}/\sqrt{s}$ and the squared center-of-mass energy is $s = 2p_A\cdot p_B$.

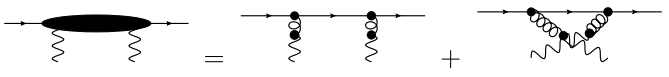

Fig. 2. Diagrams for the LO impact factor $h^{(0)}$ for quark-initiated jets. With the definitions (8), the leading order impact factors read $h_q^{(0)} = C_f^2 h^{(0)}$ and $h_g^{(0)} = C_a^2(1+\epsilon)h^{(0)}$.

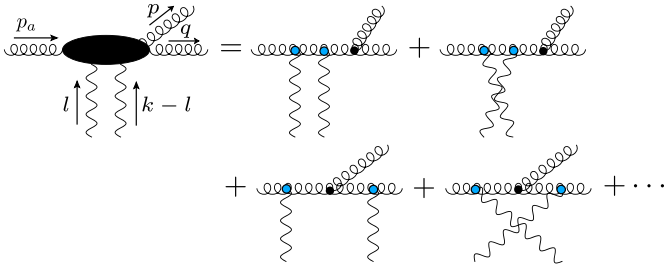

Fig. 3. Effective vertex in the quasielastic corrections to gluon-initiated jets with gg final state.

For the hadrons we write $p_A = p_A^+ n^-/2$ and $p_B = p_B^- n^+/2$, while for the jets $p_{J,i} = \sqrt{\boldsymbol{k}_{J,i}^2}(e^{y_{J,i}}n^-/2 + e^{-y_{J,i}}n^+/2) + \boldsymbol{k}_{J,i}$, $i = 1, 2$. $\boldsymbol{k}_{J,i}$ and $y_{J,i}$ are the transverse momenta and rapidity of the jets. To understand the general idea of our calculation let us point out that at LO parton level we consider the high energy limit of the process $i(p_a) + j(p_b) \to k(p_1) + l(p_2)$, with $i, j, k, l = q, \bar{q}, g$ and a color singlet exchange in the t-channel. This requires the exchange of at least two reggeized gluons. The corresponding partonic LO cross-section is

$$\frac{\mathrm{d}\hat{\sigma}_{ij}}{\mathrm{d}^2\boldsymbol{k}} = \int \mathrm{d}^2\boldsymbol{l}_1 \mathrm{d}^2\boldsymbol{l}_2 \frac{h_{i,a}^{(0)}}{\pi \boldsymbol{l}_1^2(\boldsymbol{k}-\boldsymbol{l}_1)^2}\frac{h_{j,b}^{(0)}}{\pi \boldsymbol{l}_2^2(\boldsymbol{k}-\boldsymbol{l}_2)^2}, \quad (3)$$

where $h_i^{(0)}$, $i = g, q, \bar{q}$, is the parton-two reggeized gluon vertex at LO and $\boldsymbol{k}$ the momentum transfer. Resumming $\Delta y_{\text{gap}} \sim \ln s/s_0$ terms we have

$$\frac{\mathrm{d}\hat{\sigma}_{ij}}{\mathrm{d}^2\boldsymbol{k}} = \int \frac{\mathrm{d}^2\boldsymbol{l}_1 \mathrm{d}^2\boldsymbol{l}_1'}{\pi}\frac{\mathrm{d}^2\boldsymbol{l}_2 \mathrm{d}^2\boldsymbol{l}_2'}{\pi} h_{i,a}^{(0)} h_{j,b}^{(0)} \times G\left(\boldsymbol{l}_1, \boldsymbol{l}_1', \boldsymbol{k}, \frac{s}{s_0}\right) G\left(\boldsymbol{l}_2, \boldsymbol{l}_2', \boldsymbol{k}, \frac{s}{s_0}\right), \quad (4)$$

where G is the non-forward BFKL Green function [12]. In the following we determine the NLO corrections to the parton-2 reggeized gluon couplings. They include the one-loop virtual corrections to the tree-level amplitude, already computed in [13]. The inelastic processes to be included in our calculation require the additional emission of a gluon (gluon and (anti-)quark initiated case) and splitting of the gluon into quark–antiquark pair (gluon initiated case) in the forward region of the initial state partons. We discuss them in some detail in the following.

3. Real NLO corrections to impact factors

In our framework the typical diagrams to be evaluated are shown in Figs. 2 and 3. We work in Sudakov variables for the momenta in Fig. 3: $p_a = p_a^+ n^-/2$, $k = k^- n^+/2 + \boldsymbol{k}$, $l = l^- n^+/2 + \boldsymbol{l}$, $p = (1-z)p_a^+ n^-/2 + \boldsymbol{p}^2 n^+/(2(1-z)p_a^+) + \boldsymbol{p}$, $q = zp_a^+ n^-/2 + \boldsymbol{q}^2 n^+/(2zp_a^+) + \boldsymbol{q}$. In the integration over the reggeon loop momentum we incorporate its longitudinal component into the definition of the impact factors. With the notation

$$i\{\phi_{qqg}, \phi_{ggg}, \phi_{gq\bar{q}}\} = \int \frac{\mathrm{d}l^-}{8\pi}\left\{i\mathcal{M}_{q2r^*\to qg}^{cde}, i\mathcal{M}_{g2r^*\to gg}^{abcde}, i\mathcal{M}_{g2r^*\to q\bar{q}}^{ade}\right\} P^{de}, \quad (5)$$

where $P^{de} = \delta^{de}/\sqrt{N_c^2-1}$ is the projector onto color singlet for the two-reggeon state, we can express the real contribution to the NLO correction to the impact factor, $h^{(1)}$, appearing in (4) as

$$h^{(1)}_{r,X,a}\mathrm{d}\Gamma^{(2)} = \frac{2^\epsilon}{(4\pi)^{4+3\epsilon}(p_a^+)^2}\frac{\overline{|\phi_{X,a}|^2}}{z(1-z)}\mathrm{d}\Gamma^{(2)}, \quad X=\{qqg,ggg,q\bar{q}q\}, \tag{6}$$

with $\mathrm{d}\Gamma^{(2)} = \mathrm{d}z\mathrm{d}^{2+2\epsilon}\boldsymbol{q}/\pi^{1+\epsilon}$. Associated to each forward jet, there exists a diffractive system in the forward region of the corresponding hadron, with momentum transfer $t=-\boldsymbol{k}^2$ and an invariant mass M_X. The upper limit on the latter at parton level stems from the constraint $\hat{M}_X^2 = (p_a+k)^2 < \hat{M}^2_{X,\max} = xM^2_{X,\max} + (1-x)t$ where $M_X < M_{X,\max}$ is limited by experiment and x is the momentum fraction carried by the incoming parton. We therefore find

$$\begin{aligned} h^{(1)}_{r,X}\mathrm{d}\Gamma^{(2)} = {}& \frac{h^{(0)}(1+\epsilon)}{\mu^{2\epsilon}\Gamma(1-\epsilon)}\frac{\alpha_{s,\epsilon}}{2\pi}\Theta\left(\hat{M}^2_{X,\max} - \frac{\boldsymbol{\Delta}}{z(1-z)}\right) \\ & \times\left\{\frac{1}{1+\epsilon}P_{gq}(z,\epsilon), \frac{1}{2!}P_{gg}(z,\epsilon), P_{qg}(z,\epsilon)\right\} \\ & \times J_X(\boldsymbol{q},\boldsymbol{k},\boldsymbol{l}_1,\boldsymbol{l}_2,z)\mathrm{d}\Gamma^{(2)}, \end{aligned} \tag{7}$$

where $P_{gq}(z,\epsilon) = C_f\frac{1+(1-z)^2+\epsilon z^2}{z}$, $P_{gg}(z,\epsilon) = 2C_a\frac{(1-z(1-z))^2}{z(1-z)}$ and $P_{qg}(z,\epsilon) = \frac{1}{2}(1-\frac{2z(1-z)}{1+\epsilon})$ are the real part of the Altarelli–Parisi splitting functions in $d=4+2\epsilon$ dimensions and we defined

$$\begin{aligned} &\alpha_{s,\epsilon} = \frac{g^2\mu^{2\epsilon}\Gamma(1-\epsilon)}{(4\pi)^{1+\epsilon}}, \qquad h^{(0)} = \frac{\alpha^2_{s,\epsilon}2^\epsilon}{\mu^{4\epsilon}\Gamma^2(1-\epsilon)(N_c^2-1)}, \\ &\boldsymbol{\Delta} = \boldsymbol{q} - z\boldsymbol{k}, \qquad \boldsymbol{\Sigma}_i = \boldsymbol{q} - \boldsymbol{l}_i, \qquad \boldsymbol{\Upsilon}_i = \boldsymbol{q} - \boldsymbol{k} + \boldsymbol{l}_i, \quad i=1,2, \\ &J_X(\boldsymbol{q},\boldsymbol{k},\boldsymbol{l}_1,\boldsymbol{l}_2,z) = \left[\{C_f,C_a,C_a\}\frac{\boldsymbol{\Delta}}{\boldsymbol{\Delta}^2} - \{C_f,C_a,C_f\}\frac{\boldsymbol{q}}{\boldsymbol{q}^2}\right. \\ &\quad - \{C_a,C_a,C_f\}\frac{\boldsymbol{p}}{\boldsymbol{p}^2} - \frac{1}{2}\left\{C_a,C_a,-\frac{1}{C_a}\right\} \\ &\quad \left.\times\left(\frac{\boldsymbol{\Sigma}_1}{\boldsymbol{\Sigma}_1^2} + \frac{\boldsymbol{\Upsilon}_1}{\boldsymbol{\Upsilon}_1^2}\right)\right]\cdot\left[\{1\leftrightarrow 2\}\right]. \end{aligned} \tag{8}$$

4. The NLO Mueller–Tang jet vertex

In order to define an infrared and collinear safe NLO cross section, we need to convolute the partonic cross section with a jet function S_J:

$$\frac{\mathrm{d}\hat{\sigma}_J}{\mathrm{d}J_1\mathrm{d}J_2\mathrm{d}^2\boldsymbol{k}} = \mathrm{d}\hat{\sigma}\otimes S_{J_1}S_{J_2}, \quad \mathrm{d}J_i = \mathrm{d}^{2+2\epsilon}\boldsymbol{k}_{J_i}\mathrm{d}y_{J_i}, \ i=1,2. \tag{9}$$

Infrared finiteness imposes general constraints on the jet function [14]. For two final state partons, the jet function $S^{(3)}_J(\boldsymbol{p},\boldsymbol{q},zx,x)$ must be $\{\boldsymbol{q},z\}\leftrightarrow\{\boldsymbol{p},1-z\}$ symmetric, and must reduce to the one final state parton distribution $S^{(2)}_J(\boldsymbol{p},x) = x\delta(x-|\boldsymbol{k}_J|e^{y_J}/\sqrt{s})\times\delta^{2+2\epsilon}(\boldsymbol{p}-\boldsymbol{k}_J)$ in the soft and collinear limits. In particular

$$\begin{aligned} &S^{(3)}_J(\boldsymbol{p},\boldsymbol{q},zx,x) \xrightarrow{\boldsymbol{p}\to 0} S^{(2)}_J(\boldsymbol{k},zx); \\ &S^{(3)}_J(\boldsymbol{p},\boldsymbol{q},zx,x) \xrightarrow{\frac{\boldsymbol{q}}{z}\to\frac{\boldsymbol{p}}{1-z}} S^{(2)}_J(\boldsymbol{k},x). \end{aligned} \tag{10}$$

Completing our result with the virtual corrections calculated in [13], taking into account UV renormalization of the QCD Lagrangian, and absorbing initial state collinear emissions into a redefinition of parton distribution functions, we obtain, within the collinear factorization framework, the result

$$\begin{aligned} \frac{\mathrm{d}\sigma_{J,H_1H_2}}{\mathrm{d}J_1\mathrm{d}J_2\mathrm{d}^2\boldsymbol{k}} = {}& \frac{1}{\pi^2}\int\mathrm{d}\boldsymbol{l}_1\mathrm{d}\boldsymbol{l}_1'\mathrm{d}\boldsymbol{l}_2\mathrm{d}\boldsymbol{l}_2'\frac{\mathrm{d}V(\boldsymbol{l}_1,\boldsymbol{l}_2,\boldsymbol{k},\boldsymbol{p}_{J,1},y_1,s_0)}{\mathrm{d}J_1} \\ & \times G\left(\boldsymbol{l}_1,\boldsymbol{l}_1',\boldsymbol{k},\frac{\hat{s}}{s_0}\right)G\left(\boldsymbol{l}_2,\boldsymbol{l}_2',\boldsymbol{k},\frac{\hat{s}}{s_0}\right) \\ & \times\frac{\mathrm{d}V(\boldsymbol{l}_1',\boldsymbol{l}_2',\boldsymbol{k},\boldsymbol{p}_{J,2},y_2,s_0)}{\mathrm{d}J_2}, \end{aligned} \tag{11}$$

where $\hat{s} = x_1x_2s$, $x_0 = -t/(M^2_{X,\max}-t)$ and

$$\begin{aligned} &\frac{\mathrm{d}V}{\mathrm{d}J} = \sum_{j=\{q_k,\bar{q}_k,g\}}^{k=1,\cdots,n_f}\int_{x_0}^1\mathrm{d}x\,f_{j/H}(x,\mu_F^2)\left(\frac{\mathrm{d}\hat{V}^{(0)}_j}{\mathrm{d}J} + \frac{\mathrm{d}\hat{V}^{(1)}_j}{\mathrm{d}J}\right), \\ &\frac{\mathrm{d}\hat{V}^{(0)}_j}{\mathrm{d}J} = \frac{\alpha_s^2C_j^2}{N_c^2-1}S^{(2)}_J(\boldsymbol{k},x), \\ &\frac{\mathrm{d}\hat{V}^{(1)}_j}{\mathrm{d}J} = \int d\Gamma^{(2)}\left(\frac{\mathrm{d}\hat{V}^{(1)}_{j,v}}{\mathrm{d}J} + \frac{\mathrm{d}\hat{V}^{(1)}_{j,r}}{\mathrm{d}J} + \frac{\mathrm{d}\hat{V}^{(1)}_{j,\text{UV ct.}}}{\mathrm{d}J} + \frac{\mathrm{d}\hat{V}^{(1)}_{j,\text{col. ct.}}}{\mathrm{d}J}\right), \\ &\frac{\mathrm{d}\hat{V}^{(1)}_{r,\{q_k/\bar{q}_k,g\}}}{\mathrm{d}J} = \left\{h^{(1)}_{r,qqg}, h^{(1)}_{r,q\bar{q}g} + h^{(1)}_{r,ggg}\right\}S^{(3)}_J(\boldsymbol{p},\boldsymbol{q},zx,x), \\ &\frac{\mathrm{d}\hat{V}^{(1)}_{\{q_k/\bar{q}_k,g\},\text{UV ct.}}}{\mathrm{d}J} = \left\{h^{(0)}_q, h^{(0)}_g\right\}\frac{\alpha_{s,\epsilon}}{2\pi}\frac{\beta_0}{\epsilon}S^{(2)}_J(\boldsymbol{k},x), \\ &\frac{\mathrm{d}\hat{V}^{(0)}_{\{g,q/\bar{q}\}}}{\mathrm{d}J} = h^{(0)}_{\{g,q\}}S^{(2)}_J(\boldsymbol{k},x), \\ &\frac{\mathrm{d}\hat{V}^{(1)}_{j,\text{col. ct.}}}{\mathrm{d}J} = -\frac{\alpha_{s,\epsilon}}{2\pi}\left(\frac{1}{\epsilon}+\ln\frac{\mu_F^2}{\mu^2}\right) \\ &\qquad\times\int_0^1\mathrm{d}z\,S^{(2)}_J(\boldsymbol{k},zx)\sum_{i=\{q_\ell,\bar{q}_\ell,g\}}^{\ell=1,\cdots,n_f}h^{(0)}_iP^{(0)}_{ij}(z), \end{aligned} \tag{12}$$

with $\beta_0 = \frac{11}{3}C_a - \frac{2}{3}n_f$, $P^{(0)}_{ij}(z)$ the LO DGLAP splitting functions and $C_{q,\bar{q}} = C_f, C_g = C_a$. The result for $\frac{\mathrm{d}\hat{V}^{(1)}_{j,v}}{\mathrm{d}J}$ can be extracted from [13]. Note that, when expanded to NLO, our result is independent of the scale s_0.

To write a physical representation of this vertex in dimension four we introduce a phase slicing parameter, $\lambda^2 \ll \boldsymbol{k}^2$, to regularize the singular regions in phase space. Using the limits in Eq. (10) we can rewrite $\mathrm{d}V_{q,g}/\mathrm{d}J$ in terms of λ [9] and, introducing the notations ($i=1,2$)

$$\begin{aligned} &P_0(z) = C_a\left[\frac{2(1-z)}{z} + z(1-z)\right], \\ &P_1(z) = C_a\left[\frac{2z}{[1-z]_+} + z(1-z)\right], \\ &P^{(0)}_{qq}(z) = C_f\left(\frac{1+z^2}{1-z}\right)_+, \qquad P^{(0)(z)}_{qg} = \frac{z^2+(1-z)^2}{2}, \\ &P^{(0)}_{gq}(z) = C_f\frac{1+(1-z)^2}{z}, \\ &P^{(0)}_{gg}(z) = P_0(z) + P_1(z) + \frac{\beta_0}{2}\delta(1-z), \\ &\alpha_s = \alpha_s(\mu^2), \qquad v^{(0)} = h^{(0)}\big|_{\epsilon\to 0} = \frac{\alpha_s^2}{N_c^2-1} \\ &\phi_i = \arccos\frac{\boldsymbol{l}_i\cdot(\boldsymbol{k}-\boldsymbol{l}_i)}{|\boldsymbol{l}_i||\boldsymbol{k}-\boldsymbol{l}_i|}, \end{aligned}$$

$$J_1(\boldsymbol{q},\boldsymbol{k},\boldsymbol{l}_i,z)=\frac{1}{4}\Bigg[2\frac{\boldsymbol{k}^2}{\boldsymbol{p}^2}\left(\frac{(1-z)^2}{\boldsymbol{\Delta}^2}-\frac{1}{\boldsymbol{q}^2}\right)-\frac{1}{\boldsymbol{\Sigma}_i^2}\left(\frac{(\boldsymbol{l}_i-z\boldsymbol{k})^2}{\boldsymbol{\Delta}^2}-\frac{\boldsymbol{l}_i^2}{\boldsymbol{q}^2}\right)-\frac{1}{\boldsymbol{\Upsilon}_i^2}\left(\frac{(\boldsymbol{l}_i-(1-z)\boldsymbol{k})^2}{\boldsymbol{\Delta}^2}-\frac{(\boldsymbol{l}_i-\boldsymbol{k})^2}{\boldsymbol{q}^2}\right)\Bigg],$$

$i=1,2;$

$$J_2(\boldsymbol{q},\boldsymbol{k},\boldsymbol{l}_1,\boldsymbol{l}_2)=\frac{1}{4}\Bigg[\frac{\boldsymbol{l}_1^2}{\boldsymbol{p}^2\boldsymbol{\Upsilon}_1^2}+\frac{(\boldsymbol{k}-\boldsymbol{l}_1)^2}{\boldsymbol{p}^2\boldsymbol{\Sigma}_1^2}+\frac{\boldsymbol{l}_2^2}{\boldsymbol{p}^2\boldsymbol{\Upsilon}_2^2}+\frac{(\boldsymbol{k}-\boldsymbol{l}_2)^2}{\boldsymbol{p}^2\boldsymbol{\Sigma}_2^2}-\frac{1}{2}\left(\frac{(\boldsymbol{l}_1-\boldsymbol{l}_2)^2}{\boldsymbol{\Sigma}_1^2\boldsymbol{\Sigma}_2^2}+\frac{(\boldsymbol{k}-\boldsymbol{l}_1-\boldsymbol{l}_2)^2}{\boldsymbol{\Upsilon}_1^2\boldsymbol{\Sigma}_2^2}+\frac{(\boldsymbol{k}-\boldsymbol{l}_1-\boldsymbol{l}_2)^2}{\boldsymbol{\Sigma}_1^2\boldsymbol{\Upsilon}_2^2}+\frac{(\boldsymbol{l}_1-\boldsymbol{l}_2)^2}{\boldsymbol{\Upsilon}_1^2\boldsymbol{\Upsilon}_2^2}\right)\Bigg], \tag{13}$$

we present our expression for those jets with a quark as the initial state, *i.e.*

$$\frac{\mathrm{d}\hat{V}_q^{(1)}(x,\boldsymbol{k},\boldsymbol{l}_1,\boldsymbol{l}_2;x_J,\boldsymbol{k}_J;M_{X,\max},s_0)}{\mathrm{d}J}=\nu^{(0)}\frac{\alpha_s}{2\pi}(Q_1+Q_2+Q_3)$$

$$\begin{aligned}Q_1=S_J^{(2)}(\boldsymbol{k},x)C_f^2\Bigg[&-\frac{\beta_0}{4}\Bigg\{\left[\ln\left(\frac{\boldsymbol{l}_1^2}{\mu^2}\right)+\ln\left(\frac{(\boldsymbol{l}_1-\boldsymbol{k})^2}{\mu^2}\right)+\{1\leftrightarrow 2\}\right]-\frac{20}{3}\Bigg\}-4C_f+\frac{C_a}{2}\Bigg(\Bigg\{\frac{3}{2\boldsymbol{k}^2}\Bigg[\boldsymbol{l}_1^2\ln\left(\frac{(\boldsymbol{l}_1-\boldsymbol{k})^2}{\boldsymbol{l}_1^2}\right)\\&+(\boldsymbol{l}_1-\boldsymbol{k})^2\ln\left(\frac{\boldsymbol{l}_1^2}{(\boldsymbol{l}_1-\boldsymbol{k})^2}\right)-4|\boldsymbol{l}_1||\boldsymbol{l}_1-\boldsymbol{k}|\phi_1\sin\phi_1\Bigg]-\frac{3}{2}\left[\ln\left(\frac{\boldsymbol{l}_1^2}{\boldsymbol{k}^2}\right)+\ln\left(\frac{(\boldsymbol{l}_1-\boldsymbol{k})^2}{\boldsymbol{k}^2}\right)\right]-\ln\left(\frac{\boldsymbol{l}_1^2}{\boldsymbol{k}^2}\right)\ln\left(\frac{(\boldsymbol{l}_1-\boldsymbol{k})^2}{s_0}\right)\\&-\ln\left(\frac{(\boldsymbol{l}_1-\boldsymbol{k})^2}{\boldsymbol{k}^2}\right)\ln\left(\frac{\boldsymbol{l}_1^2}{s_0}\right)-2\phi_1^2+\{1\leftrightarrow 2\}\Bigg\}+2\pi^2+\frac{14}{3}\Bigg)\Bigg],\end{aligned}$$

$$Q_2=\int_{z_0}^1\mathrm{d}z\,S_J^{(2)}(\boldsymbol{k},zx)\Bigg[\ln\frac{\lambda^2}{\mu_F^2}\left(C_f^2P_{qq}^{(0)}(z)+C_a^2P_{gq}^{(0)}(z)\right)+C_f(1-z)\left(C_f^2-\frac{2}{z}C_a^2\right)+2C_f\left(1+z^2\right)\left(\frac{\ln(1-z)}{1-z}\right)_+\Bigg],$$

$$\begin{aligned}Q_3=\int_0^1\mathrm{d}z\int\frac{\mathrm{d}^2\boldsymbol{q}}{\pi}\Bigg[&\Theta\left(\hat{M}_{X,\max}^2-\frac{(\boldsymbol{p}-z\boldsymbol{k})^2}{z(1-z)}\right)\times S_J^{(3)}\left(\boldsymbol{p},\boldsymbol{q},(1-z)x,x\right)C_f^2P_{qq}^{(0)}(z)\Theta\left(\frac{|\boldsymbol{q}|}{1-z}-\lambda^2\right)\\&\times\frac{\boldsymbol{k}^2}{\boldsymbol{q}^2(\boldsymbol{p}-z\boldsymbol{k})^2}+\Theta\left(\hat{M}_{X,\max}^2-\frac{\boldsymbol{\Delta}^2}{z(1-z)}\right)S_J^{(3)}(\boldsymbol{p},\boldsymbol{q},zx,x)\\&\times P_{gq}^{(0)}(z)\left\{C_fC_a\left[J_1(\boldsymbol{q},\boldsymbol{k},\boldsymbol{l}_1,z)+J_1(\boldsymbol{q},\boldsymbol{k},\boldsymbol{l}_2,z)\right]+C_a^2J_2(\boldsymbol{q},\boldsymbol{k},\boldsymbol{l}_1,\boldsymbol{l}_2)\Theta\left(\boldsymbol{p}^2-\lambda^2\right)\right\}\Bigg].\end{aligned} \tag{14}$$

In a similar way, the equivalent gluon-generated forward jet vertex reads

$$\frac{\mathrm{d}\hat{V}^{(1)}(x,\boldsymbol{k},\boldsymbol{l}_1,\boldsymbol{l}_2;x_J,\boldsymbol{k}_J;M_{X,\max},s_0)}{\mathrm{d}J}=\nu^{(0)}\frac{\alpha_s}{2\pi}(G_1+G_2+G_3)$$

$$\begin{aligned}G_1=C_a^2S_J^{(2)}(\boldsymbol{k},x)\Bigg[&C_a\left(\pi^2-\frac{5}{6}\right)-\beta_0\left(\ln\frac{\lambda^2}{\mu^2}-\frac{4}{3}\right)+\left(\frac{\beta_0}{4}+\frac{11C_a}{12}+\frac{n_f}{6C_a^2}\right)\left(\ln\frac{\boldsymbol{k}^4}{\boldsymbol{l}_1^2(\boldsymbol{k}-\boldsymbol{l}_1^2)}+\ln\frac{\boldsymbol{k}^4}{\boldsymbol{l}_2^2(\boldsymbol{k}-\boldsymbol{l}_2)^2}\right)\\&+\frac{1}{2}\Bigg\{C_a\left(\ln^2\frac{\boldsymbol{l}_1^2}{(\boldsymbol{k}-\boldsymbol{l}_1)^2}+\ln\frac{\boldsymbol{k}^2}{\boldsymbol{l}_1^2}\ln\frac{\boldsymbol{l}_1^2}{s_0}+\ln\frac{\boldsymbol{k}^2}{(\boldsymbol{k}-\boldsymbol{l}_1)^2}\times\ln\frac{(\boldsymbol{k}-\boldsymbol{l}_1)^2}{s_0}\right)-\left(\frac{n_f}{3C_a^2}+\frac{11C_a}{6}\right)\frac{\boldsymbol{l}_1^2-(\boldsymbol{k}-\boldsymbol{l}_1)^2}{\boldsymbol{k}^2}\\&\times\ln\frac{\boldsymbol{l}_1^2}{(\boldsymbol{k}-\boldsymbol{l}_1)^2}-2\left(\frac{n_f}{C_a^2}+4C_a\right)\frac{(\boldsymbol{l}_1^2(\boldsymbol{k}-\boldsymbol{l}_1)^2)^{\frac{1}{2}}}{\boldsymbol{k}^2}\phi_1\sin\phi_1\\&+\frac{1}{3}\left(C_a+\frac{n_f}{C_a^2}\right)\Bigg[16\frac{(\boldsymbol{l}_1^2(\boldsymbol{k}-\boldsymbol{l}_1)^2)^{\frac{3}{2}}}{(\boldsymbol{k}^2)^3}\phi_1\sin^3\phi_1-4\frac{\boldsymbol{l}_1^2(\boldsymbol{k}-\boldsymbol{l}_1)^2}{(\boldsymbol{k}^2)^2}\left(2-\frac{\boldsymbol{l}_1^2-(\boldsymbol{k}-\boldsymbol{l}_1)^2}{\boldsymbol{k}^2}\ln\frac{\boldsymbol{l}_1^2}{(\boldsymbol{k}-\boldsymbol{l}_1)^2}\right)\sin^2\phi_1\\&+\frac{(\boldsymbol{l}_1^2(\boldsymbol{k}-\boldsymbol{l}_1)^2)^{\frac{1}{2}}}{(\boldsymbol{k}^2)^2}\cos\phi_1\Bigg(4\boldsymbol{k}^2-12\left(\boldsymbol{l}_1^2(\boldsymbol{k}-\boldsymbol{l}_1)^2\right)^{\frac{1}{2}}\phi_1\sin\phi_1-\left(\boldsymbol{l}_1^2-(\boldsymbol{k}-\boldsymbol{l}_1)^2\right)\ln\frac{\boldsymbol{l}_1^2}{(\boldsymbol{k}-\boldsymbol{l}_1)^2}\Bigg)\Bigg]-2C_a\phi_1^2\\&+\{\boldsymbol{l}_1\leftrightarrow\boldsymbol{l}_2,\phi_1\leftrightarrow\phi_2\}\Bigg\}\Bigg]\end{aligned}$$

$$\begin{aligned}G_2=\int_{z_0}^1\mathrm{d}z\,S_J^{(2)}(\boldsymbol{k},zx)\Bigg\{&2n_fP_{qg}^{(0)}(z)\left(C_f^2\ln\frac{\lambda^2}{\mu_F^2}+C_a^2\ln(1-z)\right)+C_a^2P_{gg}^{(0)}(z)\ln\frac{\lambda^2}{\mu_F^2}+C_f^2n_f\\&+2C_a^3z\left((1-z)\ln(1-z)+2\left[\frac{\ln(1-z)}{1-z}\right]_+\right)\Bigg\}\end{aligned}$$

$$\begin{aligned}G_3=\int_0^1\mathrm{d}z\int\frac{\mathrm{d}^2\boldsymbol{q}}{\pi}\Bigg\{&n_fP_{qg}^{(0)}(z)\Bigg[C_a^2\Theta\left(\hat{M}_{X,\max}^2-\frac{z\boldsymbol{p}^2}{(1-z)}\right)\times S_J^{(3)}(\boldsymbol{k}-z\boldsymbol{q},z\boldsymbol{q},zx,x)\left[\frac{\Theta(\boldsymbol{p}^2-\lambda^2)\boldsymbol{k}^2}{(\boldsymbol{p}^2+\boldsymbol{q}^2)\boldsymbol{p}^2}+\frac{\boldsymbol{k}^2}{(\boldsymbol{p}^2+\boldsymbol{q}^2)\boldsymbol{q}^2}\right]\\&-\Theta\left(\hat{M}_{X,\max}^2-\frac{\boldsymbol{\Delta}^2}{z(1-z)}\right)S_J^{(3)}(\boldsymbol{p},\boldsymbol{q},zx,x)\times\left(C_a^2\frac{\boldsymbol{k}^2}{(\boldsymbol{p}^2+\boldsymbol{q}^2)\boldsymbol{q}^2}-2C_f^2\frac{\boldsymbol{k}^2\Theta(\boldsymbol{q}^2-\lambda^2)}{(\boldsymbol{p}^2+\boldsymbol{q}^2)\boldsymbol{q}^2}\right)\Bigg]\\&+P_1(z)\Theta\left(\hat{M}_{X,\max}^2-\frac{(\boldsymbol{p}-z\boldsymbol{k})^2}{z(1-z)}\right)\times S_J^{(3)}\left(\boldsymbol{p},\boldsymbol{q},(1-z)x,x\right)\frac{(1-z)^2\boldsymbol{k}^2}{(1-z)^2(\boldsymbol{p}-z\boldsymbol{k})^2+\boldsymbol{q}^2}\\&\times\left[\Theta\left(\frac{|\boldsymbol{q}|}{1-z}-\lambda\right)\frac{1}{\boldsymbol{q}^2}+\Theta\left(\frac{|\boldsymbol{p}-z\boldsymbol{k}|}{1-z}-\lambda\right)\frac{1}{(\boldsymbol{p}-z\boldsymbol{k})^2}\right]\\&+\Theta\left(\hat{M}_{X,\max}^2-\frac{\boldsymbol{\Delta}^2}{z(1-z)}\right)S_J^{(3)}(\boldsymbol{p},\boldsymbol{q},zx,x)\times\left[\frac{n_f}{C_a^2}P_{qg}^{(0)}\left(J_2(\boldsymbol{q},\boldsymbol{k},\boldsymbol{l}_1,\boldsymbol{l}_2)-\frac{\boldsymbol{k}^2}{\boldsymbol{p}^2(\boldsymbol{q}^2+\boldsymbol{p}^2)}\right)\right.\end{aligned}$$

$$
\begin{aligned}
&- n_f P_{qg}^{(0)}\big(J_1(\boldsymbol{q},\boldsymbol{k},\boldsymbol{l}_1,z) + J_1(\boldsymbol{q},\boldsymbol{k},\boldsymbol{l}_2,z)\big)\\
&+ P_0(z)\big(J_1(\boldsymbol{q},\boldsymbol{k},\boldsymbol{l}_1,z) + J_1(\boldsymbol{q},\boldsymbol{k},\boldsymbol{l}_2,z)\\
&+ J_2(\boldsymbol{q},\boldsymbol{k},\boldsymbol{l}_1,\boldsymbol{l}_2)\Theta\big(\boldsymbol{p}^2-\lambda^2\big)\big)\Big]\Big\}. \qquad (15)
\end{aligned}
$$

These expressions, although lengthy, are suited to perform phenomenological studies. It is important to note that its convolution with the nonforward BFKL Green function with exact treatment of the running of the coupling is complicated and Monte Carlo integration techniques [15] are required in order to generate exclusive distributions needed to describe different diffractive data in hadronic collisions, in particular those already recorded at the LHC.

5. Outlook

In this brief letter we have presented our final results for the jet vertex describing the coupling of a hard pomeron to a forward jet with a next-to-leading order accuracy. This result is a necessary step towards the phenomenological study of diffractive jet production at high energies. Together with the nonforward gluon Green function it allows for the study of different diffractive cross-sections with great detail, in particular when the latter is implemented in a Monte Carlo event generator [15]. Running coupling, energy scale choice and renormalization scheme issues can be addressed fully at NLO, greatly increasing the precision of our predictions.

Our procedure to use the high energy effective action proposed by Lipatov can be extended to other observables, in particular those where non-linear effects might be important. These non-linearities can be relevant already at the Large Hadron Collider and would definitely play an important role at possible future experiments such as the Large Hadron electron Collider [16].

Acknowledgements

We thank the participants of the 2nd *Informal Meeting on Scattering Amplitudes & the Multi-Regge Limit* (Madrid, February 2014) for stimulating discussions. M.H. acknowledges support from U.S. Department of Energy (DE-AC02-98CH10886) and "BNL Laboratory Directed Research & Development" grant (LDRD 12-034). J.D.M. is supported by European Research Council under Advanced Investigator Grant ERC-AD-267258. A.S.V. acknowledges support from European Commission under contract LHCPhenoNet (PITN-GA-2010-264564), Madrid Regional Government (HEPHACOS ESP-1473), Spanish Government (MICINN (FPA2010-17747)) and Spanish MINECO Centro de Excelencia Severo Ochoa Programme (SEV-2012-0249).

References

[1] G. Chachamis, M. Hentschinski, J.D. Madrigal, A. Sabio Vera, arXiv:1211.2050.
[2] L.N. Lipatov, Nucl. Phys. B 452 (1995) 369, arXiv:hep-ph/9502308;
L.N. Lipatov, Phys. Rep. 286 (1997) 131, arXiv:hep-ph/9610276.
[3] G. Chachamis, M. Hentschinski, J.D. Madrigal, A. Sabio Vera, Nucl. Phys. B 861 (2012) 133, arXiv:1202.0649.
[4] G. Chachamis, M. Hentschinski, J.D. Madrigal, A. Sabio Vera, Nucl. Phys. B 876 (2013) 453, arXiv:1307.2591.
[5] M. Hentschinski, A. Sabio Vera, Phys. Rev. D 85 (2012) 056006, arXiv:1110.6741;
G. Chachamis, M. Hentschinski, J.D. Madrigal, A. Sabio Vera, Phys. Rev. D 87 (7) (2013) 076009, arXiv:1212.4992.
[6] D. Colferai, F. Schwennsen, L. Szymanowski, S. Wallon, J. High Energy Phys. 1012 (2010) 026, arXiv:1002.1365;
B. Ducloué, L. Szymanowski, S. Wallon, Phys. Rev. Lett. 112 (2014) 082003, arXiv:1309.3229;
F. Caporale, B. Murdaca, A. Sabio Vera, C. Salas, Nucl. Phys. B 875 (2013) 134, arXiv:1305.4620;
F. Caporale, D.Y. Ivanov, B. Murdaca, A. Papa, Nucl. Phys. B 877 (2013) 73, arXiv:1211.7225;
F. Caporale, D.Y. Ivanov, B. Murdaca, A. Papa, A. Perri, J. High Energy Phys. 1202 (2012) 101, arXiv:1112.3752.
[7] V.S. Fadin, E.A. Kuraev, L.N. Lipatov, Phys. Lett. B 60 (1975) 50;
V.S. Fadin, E.A. Kuraev, L.N. Lipatov, Sov. Phys. JETP 45 (1977) 199;
L.N. Lipatov, Sov. J. Nucl. Phys. 23 (1976) 338;
Ia.Ia. Balitsky, L.N. Lipatov, Sov. J. Nucl. Phys. 28 (1978) 822.
[8] A.H. Mueller, W.-K. Tang, Phys. Lett. B 284 (1992) 123.
[9] M. Hentschinski, J.D. Madrigal, B. Murdaca, A. Sabio Vera, in preparation.
[10] E.N. Antonov, L.N. Lipatov, E.A. Kuraev, I.O. Cherednikov, Nucl. Phys. B 721 (2005) 111, arXiv:hep-ph/0411185.
[11] M. Hentschinski, The high energy behavior of QCD: the effective action and the triple-Pomeron-vertex, PhD thesis, Hamburg University, 2009, arXiv:0908.2576;
M. Hentschinski, Nucl. Phys. B 859 (2012) 129, arXiv:1112.4509.
[12] V.S. Fadin, R. Fiore, Phys. Rev. D 72 (2005) 014018, arXiv:hep-ph/0502045;
V.S. Fadin, R. Fiore, A. Papa, Nucl. Phys. B 865 (2012) 67, arXiv:1206.5596.
[13] V.S. Fadin, R. Fiore, M.I. Kotsky, A. Papa, Phys. Rev. D 61 (2000) 094006, arXiv:hep-ph/9908265;
V.S. Fadin, R. Fiore, M.I. Kotsky, A. Papa, Phys. Rev. D 61 (2000) 094005, arXiv:hep-ph/9908264.
[14] S. Catani, M.H. Seymour, Nucl. Phys. B 485 (1997) 291, arXiv:hep-ph/9605323;
S. Catani, M.H. Seymour, Nucl. Phys. B 510 (1998) 503 (Erratum).
[15] G. Chachamis, M. Deak, A. Sabio Vera, P. Stephens, Nucl. Phys. B 849 (2011) 28, arXiv:1102.1890;
G. Chachamis, A. Sabio Vera, Phys. Lett. B 709 (2012) 301, arXiv:1112.4162;
G. Chachamis, A. Sabio Vera, Phys. Lett. B 717 (2012) 458, arXiv:1206.3140;
G. Chachamis, A. Sabio Vera, C. Salas, Phys. Rev. D 87 (2013) 016007, arXiv:1211.6332.
[16] J.L. Abelleira Fernandez, et al., LHeC Study Group Collaboration, J. Phys. G 39 (2012) 075001, arXiv:1206.2913.